Energy 252 (2022) 123919

Contents lists available at ScienceDirect

Energy

journal homepage: www.elsevier.com/locate/energy

Co-combustion characteristics and CO_2 emissions of low-calorific multi-fuels by TG-FTIR analysis

Zhangke Ma, Leming Cheng*, Qinhui Wang, Liyao Li, Guanwen Luo, Weiguo Zhang

Institute for Thermal Power Engineering, State Key Laboratory of Clean Energy Utilization, Zhejiang University, Hangzhou, Zhejiang, 310027, China

ARTICLE INFO

Article history:
Received 22 December 2021
Received in revised form
31 March 2022
Accepted 2 April 2022
Available online 20 April 2022

Keywords:
CFB
Co-combustion
Carbon dioxide emission
Coal slime
Coal gangue
TG-FTIR

ABSTRACT

In this study, the combustion performance and CO_2 emission of coal slime (CS), coal gangue (CG) and raw coal (RC) mixtures were systematically investigated by TG-FTIR. The interaction and kinetics during the co-combustion process were analyzed. The results show that the co-combustion avoids the drawbacks of mono-combustion and is conducive to reduce the emission of CO_2. The effects of proportion in the blends, O_2 concentration and heating rate were discussed and the optimum combustion parameters are obtained by the orthogonal experiments. As the proportion of CS increases in the mixtures, the average comprehensive combustion characteristic index (S_{ave}) increases by 2.1 times. Synergistic interaction is detected between CS, CG and RC during co-combustion. Moreover, the CO_2 absorption peak of CS is much higher than that of CG and RC. By mixing method, the experimental CO_2 integral values are about 50% lower than anticipated. In order to get better combustion characteristics and lower CO_2 emission, the potential global optimum blending ratio of CS is 80%, O_2 concentration and heating rate for co-combustion of the mixtures are 40% and 30 °C/min, respectively. This study provides valuable information for the proportion selection and optimization of co-combustion system of coal blends in the CFB.

1. Introduction

The fossil energy for electricity production has been widely developed in circulating fluidized bed boiler (CFBB) plants in China. Under a high clean energy scenario, the disposal of low heat value coals gains a considerable momentum due to its increasing generation and consequent environmental pollution [1]. Coal slime (CS) is a semi-solid composed of fine coal particles, moisture and impurities [2]. It is characterized by low heat value (8–17 MJ/kg), small particle size (<1 mm) and high moisture (20%–50%) [3]. Coal gangue (CG) is an abandoned carbonaceous rock and reserves approach 70 billion tons [4]. It has the features of low volatile, high ash and low heat value [5]. In the recent decades, the utilizations of CS and CG in technology have been developed in combustion, liquidation, gasification and pyrolysis [6]. Combustion technology stands out from the numerous methods due to its high energy efficiency and low operation cost [7]. It is beneficial to realize energy recycling and pollution control of CS and CG.

The circulating fluidized bed (CFB) combustion technology is one of the best selections to use those low heating value coals, owing to the advantages of low combustion temperature, wide fuel adaptability and low pollutant emission [8]. Co-combustion is defined as the combustion of two or more different types of fuel burning in the same furnace at the same time. It is an effective method to increase fuel flexibility, improve the performance of coals, extend the range of acceptable coals, and meet specifications of power plants [9]. Duan et al. [10] found the co-combustion and boiler efficiency could be improved in a 75 t/h CFB boiler using coal slime and medium coal. Fu et al. [11] pointed out that adding sewage sludge into coal slime would improve combustion performance and reduce the arsenic release. The blended-coal co-combustion technology improves energy utilization and power generation efficiency. Of these factors, the co-combustion in CFB is a promising method for low heating value blended-coal to both promote the limits of original pollutant emission of CO_2 and ensure the boiler thermal efficiency.

There are studies of combustion behavior of coal slime and coal gangue at present [12,13]. They are discussed in two groups, i.e. mono-combustion (single type of fuel) [5] and co-combustion (two or more types of fuel) [12]. Various mono-combustion researches, including mathematical simulation and measurement in the fluidized bed are briefly investigated, whereas for co-combustion,

* Corresponding author.
E-mail address: lemingc@zju.edu.cn (L. Cheng).

https://doi.org/10.1016/j.energy.2022.123919
0360-5442/

attention has been given to coal combustion with sewage sludge [14], biomass [15] and refuse-derived fuel [16] in CFB boilers, as well as synergistic effects during the co-processing. The main drawback of mono-combustion of coal slime is ignition problem due to agglomeration and cracking [17]. Fan et al. [18] reported the surface temperature of the single slime dough only reached 200 °C when it was injected into a 900 °C furnace. Loboda et al. [19] proposed that the time of slime ignition was determined by processes of drying, pyrolysis, oxidation of carbon, as well as moisture content. Similar conclusions were drawn that the ignition delay and burnout time of coal slime increased with the growing particle size [20]. Omar et al. [21] investigated the combustion characteristics of high-ash coal slime in an atmospheric fluidized-bed combustor at bed temperatures of 750–850 °C. They found that combustion of single coal slime was improper because of low boiler efficiency and high pollutant emissions. Similarly, it was difficult for coal gangue to be used as a single fuel in a CFB boiler due to its low volatile content, high ash and sulfur content. The comprehensive burnout index (R_j) related to peak temperature and burnout time was proposed by Song et al. [22]. They concluded that R_j decreased with the increment of particle size of gangue. The increment of the heating rate led to an intensified combustion reaction rate as well as increases of the ignition temperature and burnout temperature.

The drawback in combustion of individual coal slime and coal gangue has attracted the attention of researchers. Some literatures concentrated on co-combustion behaviors of multi-fuels regarding ignition, burnout, flue gases emissions, and so on. Thermogravimetric analysis is the common technique used to investigate thermal events and kinetics during the combustion of solid materials [23]. It has been confirmed that the conclusions drawn by thermogravimetry can provide an important reference for operation of a boiler firing blended coal [24]. Some studies have been conducted to investigate the effects of heating rate, oxygen concentration, mixed ratio, etc. For example, Cheng et al. [25] found that increasing the heating rate and the concentration of oxygen both contributed to the burning of raw coal/coal slime, and the influence of oxygen concentration on coal slime was more obvious than raw coal. Jiang et al. [26] showed that the main combustion characteristic parameters decreased with increasing the coal slime ratio in coal but improved as the oxygen concentration increased. Moreover, some researchers pointed out that the co-combustion process is often not a linear superposition of a single fuel. There are synergetic interactions between fuels with different characteristics. The presence of synergy and its intensity are dependent on the physical/chemical properties of the fuels, affecting the overall combustion process. Some studies have found that interactions between the component coals during combustion influenced by the particle size, blend ratio, operating conditions and so on. Liao et al. [27] reported that promotive synergy appeared during the co-combustion of coal slime, coal gangue and slack coal. The promotion became stronger as the proportion of coal gangue or slack coal increased. Oladejo et al. [28] observed that the synergistic effects during the co-combustion processing of coal and biomass were associated to biomass constituents.

Although the previous works have indicated the synergistic interaction between coal slime, coal gangue and other fuels such as coal and biomass, the co-combustion characters of low heat value multi-fuel such as raw coal, coal slime and coal gangue for CFB combustion have not attracted a wide interest. As mentioned above, the combustion characteristics of raw coal, coal slime and coal gangue are quite different, due to their fuel property diversity. The operating conditions of raw coal, coal slime and coal gangue have significant effect on the combustion parameters, i.e. combustion behaviors, kinetics, and CO_2 release characteristics. To the best of our knowledge, these properties also affect the operation of CFB boilers and flue gas pollutant control. Particularly, CO_2 emission characteristics during combustion of multi-fuel including coal, coal slime and coal gangue need to be studied under the global CO_2 control background, which is still very insufficient in recent investigations.

The goal of this work is to investigate the co-combustion performance and CO_2 emission of coal slime, coal gangue and raw coal blends. For this purpose, the thermogravimetric (TG) integrated with a Fourier-transform infrared (FTIR) technique was used. In this article, research on blended coals is systematic and comprehensive, including combustion characteristics, interaction, kinetics and gaseous emission. To gain the optimal operating conditions, the effects of proportion of CS in the blends, O_2 concentration and heating rate were discussed by orthogonal experiments. Meanwhile, the synergistic interaction between CS, CG and RC and the kinetic parameters during the co-combustion process were investigated. Two main parameters-the comprehensive combustion index (S) and the CO_2 integral value of per unit calorific (I/Q) were used which best represent the co-combustion characteristics and CO_2 emission of the CS, CG and RC blends. The research results are expected to provide valuable data for low-calorific multi-fuels combustion in CFB.

2. Experimental method

2.1. Materials

The samples of coal slime (CS), coal gangue (CG) and raw coal (RC) investigated in this study were dried at 105 °C for 24 h. Then, they were milled and sieved into a particle size of <178 μm. Table 1 shows the proximate analyses, ultimate analyses and low heat values (LHV) of CS, CG and RC. RC possessed highest volatile content (12.13%) which was conducive to the improvement of in ignition. The high ash content (66.84%) in CG hindered the mass transfer but catalyzed the combustion of fixed carbon. In addition, the LHV of CG was 6.56 MJ/kg, which was much lower than that of CS (14.64 MJ/kg). Above all, there were complementary basic characteristics in multi-fuels, which might contribute in the cooperative combustion.

2.2. TG-FTIR analysis

The co-combustion performance of CS, CG and RC and their mixtures was investigated in a thermogravimetric (TG, with a resolution of 0.01%) apparatus (NETZSCH STA449F3) coupled with a Fourier-transform infrared (FTIR) spectrometer (BRUKER Tensor 27, with a resolution of 4 cm^{-1}), as shown in Fig. 1. First, CS, CG and RC were mechanically mixed in the desired proportions. During each test, the TG-FTIR baseline was corrected by predetermined baselines, except for the addition of sample. Then, about 10 g sample was measured by a Mettler Toledo-XS105DU electronic balance (with a resolution of 0.1 mg) and preheated at a heating rate of 20 °C/min under a protective atmosphere of high purity nitrogen. When the temperature reached 50 °C, the atmosphere was switched to a reactive atmosphere of 21–60 vol% O_2/N_2 balance. Subsequently, the samples were heated from 50 °C to 1000 °C at 10–30 °C/min. In this stage, the mass change and gaseous products of sample were detected by TG-FTIR and recorded in a computer. The total flow rate during co-combustion process was kept at 50 mL/min. The spectral wavenumber range of FTIR was 600–4000 cm^{-1}. The measurement accuracy of FTIR for the gaseous products is ±3%.

Ignition temperature (T_i), burnout temperature (T_f) and comprehensive combustion characteristic index (S) were adopted to assess the co-combustion characteristics of fuel particles [29]. T_i

Table 1
Proximate and ultimate analyses of CS, CG and RC.

Samples	Proximate analysis (wt.%)				Ultimate analyses (wt.%)					LHV (MJ/kg)
	M_{ar}	A_{ar}	V_{ar}	FC_{ar}	C_{ar}	H_{ar}	N_{ar}	S_{ar}	O_{ar}	Q
RC	7.38	49.37	12.13	31.12	34.89	1.98	0.73	2.57	3.08	11.67
CS	23.24	29.6	6.83	40.33	42.5	1.41	0.64	0.52	2.09	14.64
CG	2.41	66.84	11.4	19.35	22.69	1.51	0.61	3.54	2.4	6.56

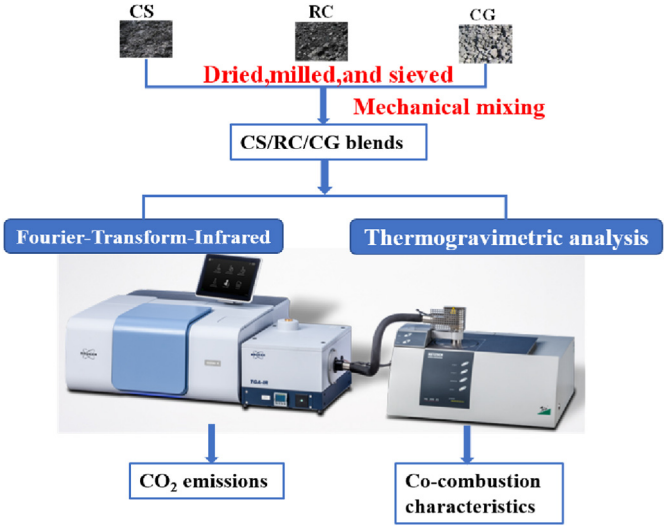

Fig. 1. Schematic of the experimental approach and devices.

was obtained by tangent method of TG and DTG curves. According to literature [30], the ignition temperature was determined based on the temperature at which the DTG had its peak value and the corresponding slope to the intersection with respect to the TG profile. T_f was delimited as the temperature corresponding to the 1%/min mass reduction rate of DTG curve at the end of combustion process [31]. S is commonly used to comprehensively quantify the combustion characteristic of the samples. The combustion reactivity of sample is considered directly proportional to the maximum and average rate of mass loss (DTG_{max} and DTG_{mean}), whereas it is inversely proportional to the ignition temperature (T_i) and burnout temperature (T_f). The use of these four values in a parameter provides an average of fuel reactivity, S. According to Fan [32], a higher S corresponds to better combustion behavior which was calculated by Eq. (1):

$$S = \frac{DTG_{max} DTG_{mean}}{T_i^2 T_f} \tag{1}$$

where, T_i is the ignition temperature, °C; T_f is the burnout temperature, °C; DTG_{max} and DTG_{mean} represent the maximum and average mass reduction rate, respectively, %/min.

The uncertainty of the measurement result was mainly caused by the mass loss measurement of the sample. Thus, each group of experiments was repeated three times, and every measurement result was recorded. For this work, two sources of uncertainty in the measurement were considered: the accuracy of the TG analyzer and the repeatability of the experiment. In particular, the accuracy of the TG analyzer was ±0.01%, and the standard uncertainty due to the resolution of the accuracy of the analyzer was ±0.0001%, which can be neglected in this uncertainty analysis. The uncertainty due to the measurement repeatability was the standard deviation of the mean of the repeat experiment, and the standard deviation of the mass measurement was ±0.0527%. According to Eq. (1), the uncertainties of comprehensive combustion index was $\pm 0.0083\%^2 \cdot min^{-2} \cdot °C^{-3}$. This illustrated that this experiment had good repeatability. In addition, the average value of the three experiments was used as the final value and shown in the results and discussion section.

2.3. Orthogonal experiments

In order to obtain the optimal combustion parameters, the orthogonal experiments were designed based on limited tests [33]. As shown in Table 2, three impact factors (proportion of CS, O_2 concentration and heating rate) were detected and each factor has three or four levels, the orthogonal matrix is adopted to obtain the optimal level of these factors. The numbers are listed from 1 to 12, representing the 12 cases. As far as we known, elevated oxygen level leads to faster burning and earlier release of CO_2 during coal combustion. However, when O_2 concentration gets too high, its effect will become feeble. Likewise, low O_2 concentration is inadequate for coal combustion progress to grow to the maximum rate [34]. Thus, high percentages of O_2 (40, 60 vol%) were adopted for an oxygen-enriched air environment, with the remainder composed of N_2. Also, a 21%O_2/79%N_2 mixture was used as a reference. The RC/CG were mixed with CS at the weight ratios of 20%,40%, 60%, 80% (expressed as CS:RC:CG = 80:10:10, 60:20:20, 40:30:30, 20:40:40). More blending ratios of CS, RC, CG in the mixtures may be analyzed for further experiment. R_i was calculated to describe the effect degree of each factor, as follow [35]:

$$R_i = d\left|\max\left(\frac{\sum_{j=1}^{L_i} S_{(i,j)}}{L_i}\right) - \min\left(\frac{\sum_{j=1}^{L_i} S_{(i,j)}}{L_i}\right)\right| \tag{2}$$

where, R_i is the effect index of each factor in range analysis; i is the factor; j is the level of each factor; L_i is the number of level for i factor; d is the coefficient, 0.45 for 4 levels and 0.52 for 3 levels; $S_{(i,j)}$ is the comprehensive combustion characteristic index of the sample for i factor j level.

Table 2
Design of orthogonal experiments for co-combustion between CS, CG and RC.

Run No.	Proportion of CS (%)	O_2 concentration (%)	Heating rate (°C/min)
1	20	21	10
2	40	40	10
3	60	60	10
4	80	60	20
5	80	40	30
6	60	21	30
7	40	21	20
8	20	60	30
9	20	40	20
10	40	60	30
11	60	40	20
12	80	21	10

2.4. Kinetic analysis

The Coats-Redfern integration method was adopted for kinetic analysis based on single rate scanning curves measured at each testing conditions [36].As a typical model-based method, a mechanism function $f(\alpha)$ need to be introduced and a fair-weather value of the activation energy can be obtained. The basic equation was shown as follow:

$$\frac{d\alpha}{dt}=\frac{A}{\beta}\exp\left(-\frac{E}{RT}\right)f(\alpha) \tag{3}$$

where, α is the mass conversion degree, %; A is the pre-exponential factor, min^{-1}; β is the heating rate, °C/min; R is the universal gas constant, 8.314 J/(mol·°C); T is the absolute temperature, °C; $f(\alpha)$ is the mechanism function. E is the activation energy, J/mol; The conversion degree α was described by:

$$\alpha=(m0-mt)/(m0-m1) \tag{4}$$

where, m_0 and m_1 denote the initial mass and the final mass of the sample, respectively. m_t represents the mass of the samples at time t. In order to accurately suit the experimental data of TG-DTG, four α (0.2, 0.4, 0.6 and 0.8) are adopted to obtain the activation energy. In this paper, the kinetics were discussed at temperature ranges of 400–650 °C, and the kinetic function 1-α is considered as the most probable reaction mechanism [26]. According to Coats-Redfern method, Eq. (3) can be transformed as follow:

$$\ln\left(\frac{-\ln(1-\alpha)}{T^2}\right)=\ln\frac{AR}{\beta E}-\frac{E}{RT} \tag{5}$$

For β is constant (10, 20, 30 °C/min), E was estimated from the slope of the straight line by plotting ln (-ln (1-α)/T^2) vs. 1/T.

3. Results and discussion

3.1. TG analysis of CS, CG, RC and the mixtures

3.1.1. TG analysis of CS, CG, RC

To compare the combustion performance of individual fuels, combustion experiments of CS, CG and RC were carried out separately. Fig. 2 presents the TG and DTG curves of CS, CG and RC at 20 °C/min. During the initial heating process, the TG curves slightly rises, which is due to the chemical adsorption of oxygen on the surface of samples. It can be found that there is only one noticeable mass loss peak in the DTG curves of RC and CS, and the major stage extends from 350 °C to 650 °C where is mainly the release of volatile matter and combustion of fixed carbon in samples. The comparisons of this stage are listed as follows: mass losses of RC and CS are about 47% and 60%, respectively. The maximum weight loss rate of CS (12.4%/min) is 75% higher than that of RC (7.1%/min). But unlike the DTG curves of RC and CS, there are two mass loss peaks in the combustion of CG, as shown in Fig. 2. The two mass loss peaks of CG occur at the temperature range of 350–650 °C and 700–800 °C which divide the CG combustion process into two major stages. One is related to the combustion of volatile matter and char, the other is due to the decomposition of minerals such as aluminosilicate contained in the CG [5]. In addition, the combustion residues of their own initial mass of CS, RC and CG are 38.5%, 50.6% and 51.3%, respectively. These statistics show that RC and CG contain more noncombustible materials such as ash and other minerals. Therefore, adding more CS into RC and CG may ameliorate the combustion characteristics of RC and CG.

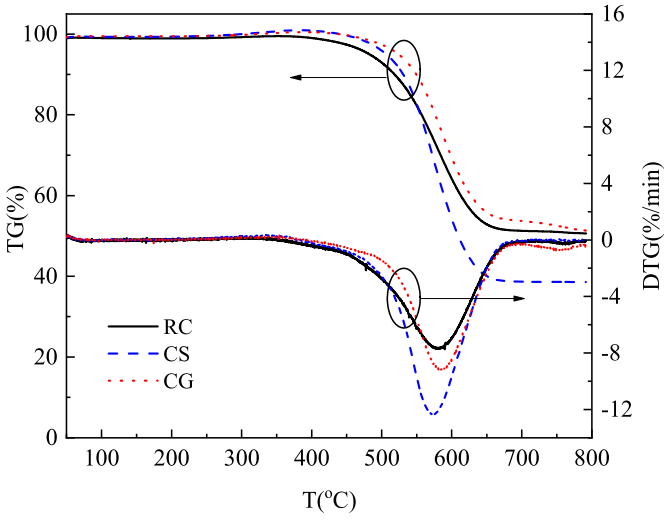

Fig. 2. The TG and DTG curves of CS, CG and RC.

The combustion characteristic parameters for individual CS, CG, RC are listed in Table 3. The ignition temperature of RC is 507.6 °C, which is 17 and 28 °C lower than that of CS and CG, respectively. The burnout temperatures of RC (768.5 °C) and CG (788.8 °C) are 78 and 98 °C higher than that of CS (690.2 °C), respectively. The ignition temperature is concerned to the volatile content in the fuel. Generally, higher volatile content is beneficial for ignition. Although the fixed carbon content in the CG is low, the high ash content contributes to long burnout time. Besides, S of CS is much higher than that of RC and CG, which is mainly due to the high LHV and low ash content of CS (as shown in Table 1).

3.1.2. TG analysis of mixtures of CS, CG, RC

The TG and DTG curves of RC, CS and CG mixtures under mass ratio of 50:50 are shown in Fig. 3. There exists the second stage of the blends extends from 700 to 800 °C when adding CG into CS and RC, which is mainly considered as the decomposition of mineral matter in the blends. The maximum weight loss peaks of mixtures are higher than that of individual RC and CG, corresponding to the reduction of ash content in the mixtures. Table 4 displays the characteristic parameters of mixed samples. It is shown that all the co-combustion parameters of blends lay between the individual samples. Compared with RC and CG, combustion performance of their blends is significantly improved. For example, the ignition temperature of RC:CG = 50:50 is 10 °C lower than that of CG, the burnout temperatures of CS:CG = 50:50 is 27 °C lower than that of CG. These indicate that co-combustion is benefit for promoting ignition and burnout performance and thermal reactivity.

3.1.3. Orthogonal experiments on combustion performance of mixtures of CS, CG and RC

Fig. 4 illustrates the effects of proportion of CS, O_2 concentration and heating rate on the combustion of CS, CG and RC blends based on the orthogonal experiments. The average comprehensive combustion characteristic index (S_{ave}) of the sample for each level are calculated by Eq. (6):

$$S_{ave}=\frac{\sum_{j=1}^{L_i}S_{(i,j)}}{L_i} \tag{6}$$

where, i is the influential factor; j is the level of each factor; $S_{(i,j)}$ is the comprehensive combustion characteristic index of the sample for i factor j level.

With the increasing addition of CS from 20% to 80%, S_{ave}

Table 3
Characteristic parameters for CS, CG, RC.

Samples	T_i (°C)	T_f (°C)	DTG_{max} (%·min^{-1})	DTG_{mean} (%·min^{-1})	$S \times 10^7$ (%^{2}·min^{-2}·°C^{-3})
RC	507.6	768.5	7.74	1.29	0.50
CS	524.4	690.2	12.43	1.62	1.06
CG	535.0	788.8	9.25	1.28	0.52

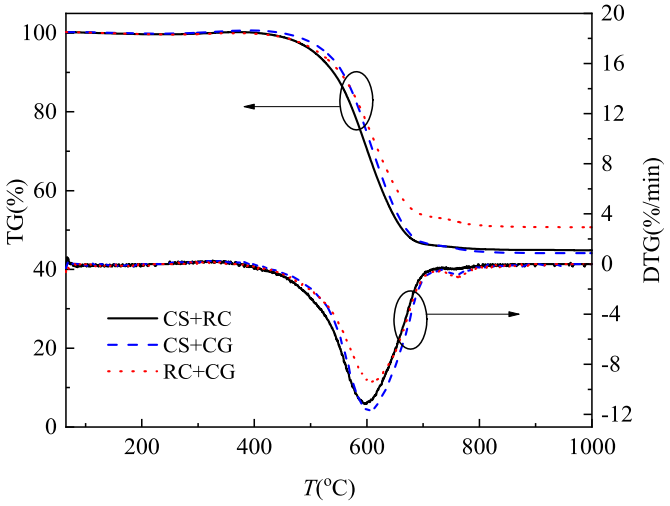

Fig. 3. TG and DTG curves for blends of CS, CG, RC.

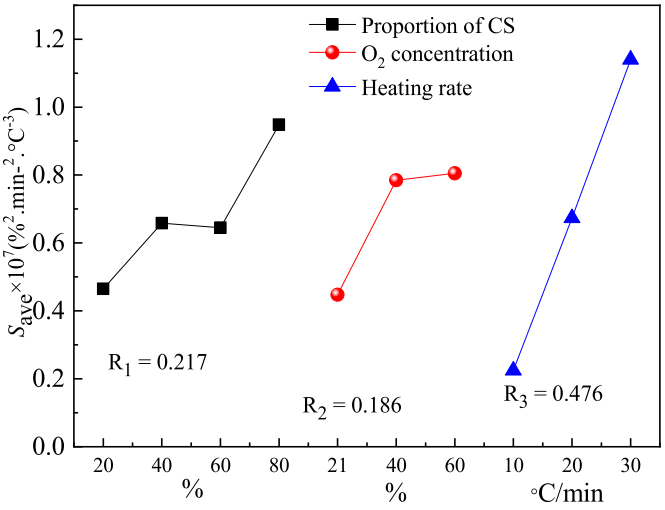

Fig. 4. Orthogonal experiments on combustion performance of blends of CS, CG and RC.

increases by 2.1 times. This is due to the high combustible content in CS and the existence of weak chemical bond strength of structure, which can be released and decomposed during combustion. As the O_2 concentration increases from 21% to 40%, S_{ave} increases by 75% due to improvement in coal combustion reactivity. With increasing O_2 concentration from 40% to 60% further, S_{ave} increases by 3%. In application of co-combustion of CS, RC and CG in a fluidized bed, a higher oxygen concentration may be considered as a good choice because of decreasing the heat absorbed by fluidization air and improving the combustion stability. As the heating rate increases, S_{ave} becomes correspondingly higher. This is because the coal particles are impacted by a strong updraft, accelerating the reaction with oxygen and increasing the combustion intensity. Based on the average comprehensive combustion characteristic index in Fig.4, 80%, 40% and 30 °C/min are the optimum levels for the proportion of CS, O_2 concentration and heating rate, respectively. A higher R_i means the stronger effect of the factor *i*. According to R_i, the heating rate has a stronger influence on the combustion characteristics of the blends than the other factors.

3.2. Synergistic interaction and kinetic analysis

3.2.1. Analysis of synergies

A deviation of experimental and theoretical values of TG or DTG reveals the presence of synergistic interaction between each other [37]. In this work, the theoretical DTG curves of RC, CS and CG blends under mass ratio of 50:50 are compared with the experimental values. The theoretical DTG values of the blends were calculated according to linear superposition of single coal, i.e.:

$$DTG_{blend} = x_1 DTG_{RC} + x_2 DTG_{CS} + x_3 DTG_{CG} \quad (7)$$

where, DTG_{RC}, DTG_{CS} and DTG_{CG} are the experimental reaction rates of the individual fuels; x_1, x_2 and x_3 are the ratios of RC, CS and CG in the blend, respectively; DTG_{blend} donates the calculated reaction rate of the mixture.

As shown in Fig. 5, the experimental and calculated curves of the blends exhibit a similar tendency throughout the combustion stage with some partial deviations. At the beginning and end of co-combustion, the two curves present a high extent of coincidence, indicating the absence of interaction between each two samples. This is due to the high ignition temperature (above 500 °C) and high burnout temperature (above 700 °C) of these three coals. However, the deviation of the theoretical and experimental DTG curves in the temperature range of 450–700 °C was clear, which was manifested in the rise of maximum mass loss rate. The experimental values of maximum mass loss rate are significantly larger than that of the theoretical values. This reveals that there is positive synergistic interaction between RC, CS and CG during the co-processing of intense combustion [38,39]. These interactions are responsible for the overall non-additive combustion behavior of blended coals. The promotive effect is due to the devolatilization of the higher-volatile coal during its volatile preferentially releasing

Table 4
Characteristic parameters for blends of CS, CG, RC.

Samples	T_i (°C)	T_f (°C)	DTG_{max} (%·min^{-1})	DTG_{mean} (%·min^{-1})	$S \times 10^7$ (%^{2}·min^{-2}·°C^{-3})
CS + RC (50:50)	519.2	729.0	11.73	1.59	0.95
CS + CG (50:50)	531.0	761.6	11.16	1.56	0.81
RC + CG (50:50)	525.2	773.3	9.45	1.40	0.62

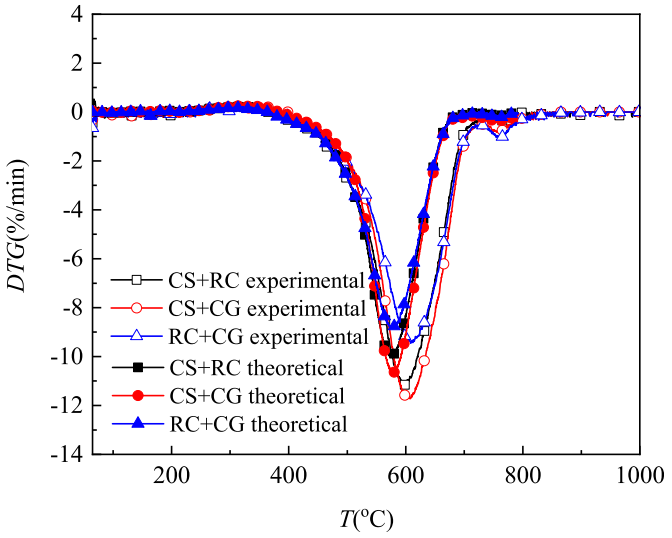

Fig. 5. Comparison between the experimental and theoretical reaction rate curves for the RC, CS and CG blends.

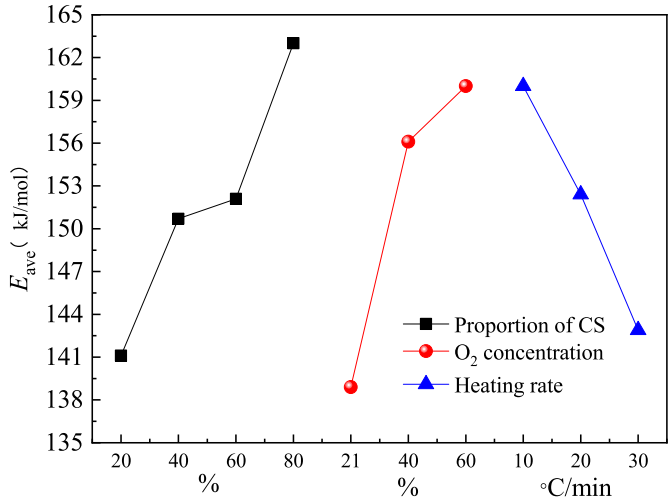

Fig. 6. Average activation energy of the samples.

and burning to form a higher gas temperature environment [40]. This promotes the devolatilization and ignition of the less-volatile coal. As for the three coal samples in this work, the RC possesses the highest volatile content (12.13%) which is considered as a flammable coal. The ash matter of CG is significantly higher than that of RC and CS, which is rich of Fe_2O_3 and other active mineral substances [41]. Therefore, in the co-firing process of CS, RC and CG, the volatile matter in the RC is separated initially, releasing heat to promote the ignition of the CS and RC. At the same time, the active minerals in the CG promote the combustion process of the RC and CS in turn. Particularly, in the temperature range of 600–700 °C, which mainly at the combustion stage of fixed carbon, the experimental values are much larger than the calculated values. This indicates the promoting effects are more prominent. It can be attributed to enlarged particles interspace and mitigated hinder of ash which are beneficial to improve the combustion performance of fixed carbon. To sum up, the synergistic interactions influence the non-additive combustion behavior of different compositions.

3.2.2. Kinetic parameters

The co-combustion characteristic of multi-fuels with complex reaction mechanism were attributed to the complicated components in RC, CS and CG blends. Thus, the global kinetic parameters of different samples were accurately calculated by using Coats-Redfern method. Based on Eq. (5), the experimental activation energy (*E*-exp) of RC, CS, CG and their blends were calculated, as shown in Table 5. The activation energy of RC is 105.9 kJ/mol, which is lower than that of CS and CG. This is mainly related to the higher volatile content in the RC. The activation energy of blends of RC, CS and CG is between 105.9 and 154.4 kJ/mol. The theoretical value *E*-cal is linearly superimposed according to the blending ratio. It can be found that *E*-exp of each mixed fuel is lower than *E*-cal, which further illustrates that there is positive synergistic interaction in the co-combustion process, and the interaction reduces the activation energy and improves the combustion performance of blends.

Table 5
The kinetic parameters of RC, CS, CG co-combustion.

Samples	*E*-exp (kJ/mol)	*E*-cal (kJ/mol)
RC	105.9	–
CS	154.4	–
CG	154.2	–
CS + RC (50:50)	116.9	130.2
CS + CG (50:50)	128.1	154.3
RC + CG (50:50)	107.3	130.1

The average activation energies for the samples at different experimental conditions are shown in Fig. 6. The average activation energy (E_{ave}) of the sample for each level are calculated by Eq. (8):

$$E_{ave} = \frac{\sum_{j=1}^{L_i} E_{(i,j)}}{L_i} \tag{8}$$

where, *i* is the influential factor; *j* is the level of each factor; $E_{(i,j)}$ is the activation energy of the sample for *i* factor *j* level, kJ/mol. It can be seen in Fig. 6 that as the proportion of CS in the mixture increases from 20% to 80%, the activation energy of the sample increases. In addition, with the growth of O_2 concentration from 21% to 40%, E_{ave} increase sharply. It is worth noting that there is a rapid fall of the average activation energy with the rise of heating rate. Because higher heating rate can promote combustion reaction, it should correspond to lower activation energy.

3.3. CO_2 emission characteristics during co-combustion process

TG coupled with FTIR is a necessary and valuable method in in-depth investigating combustion of coals, as it monitored continuously both the weight of samples and the evolution of the gas products such as CO_2. The gaseous product can be qualitatively analyzed by the relative size of the absorption peak and absorbance. Also, the relationship between the amount of CO_2 and its change with temperature can be distinguished during the co-combustion process of the blends. Fig. 7 is a three-dimensional infrared absorption diagram of the gaseous products obtained from combustion of RC, CS and CG. Comparing with the results of thermogravimetric analysis, the release of the gaseous products is associated with the decomposition stages of the samples.

Based on the main weight loss stages of each sample, four maxima of production of gases in the combustion process are discovered from the IR spectrum, as plotted in Fig. 8. The IR spectrums of RC, CS, CG are obtained based on the peak absorbance observed at the relative temperature of 580 °C (RC), 572 °C (CS), and 588 °C (CG), respectively. It can be seen that the IR spectrums of the three samples exist maximum absorbance in the wavenumber

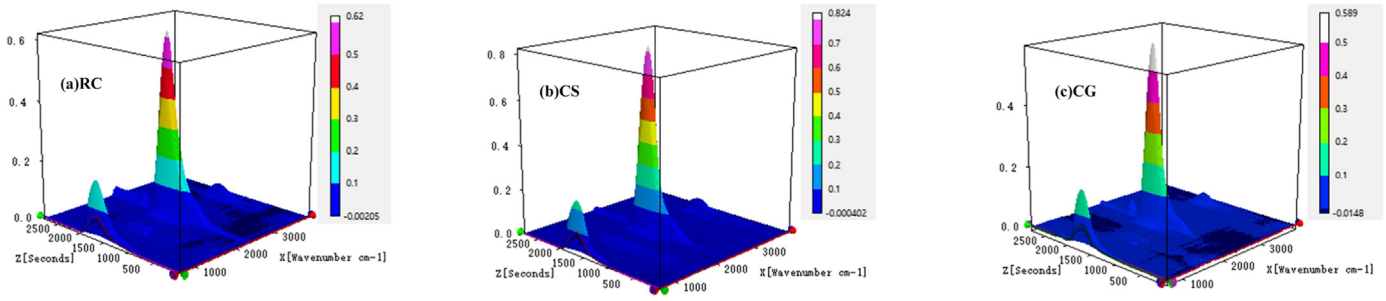

Fig. 7. Three-dimensional IR spectrum of the gas products obtained from combustion of RC, CS and CG.

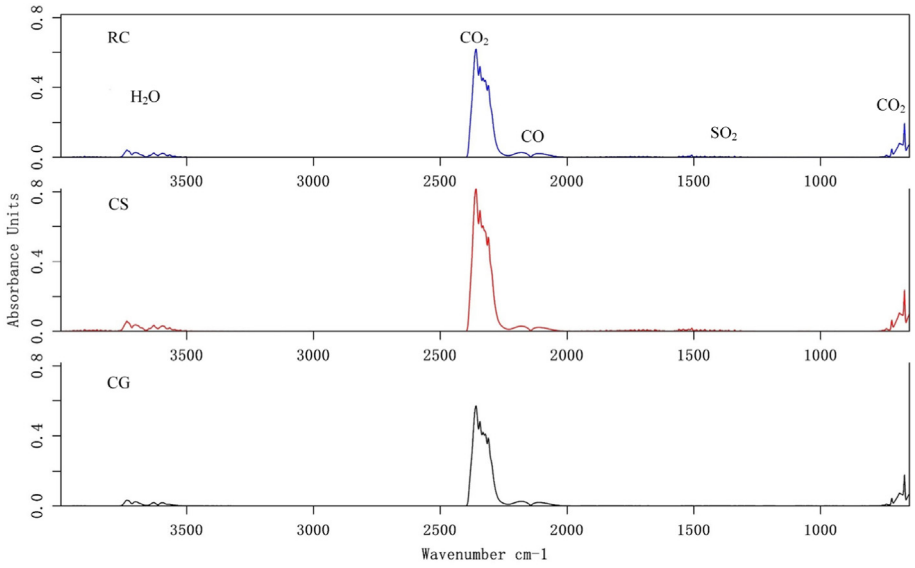

Fig. 8. IR spectrum of the gas products obtained from combustion of RC, CS and CG at several selected temperatures according to TG analysis.

range of 2400–2240 cm^{-1} and 780-560 cm^{-1} that both corresponding to CO_2, which is attributed to the devolatilization and char combustion. Additionally, the intensity of CO_2 in the region of 2400–2240 cm^{-1} of CS is higher than that of RC and CG, suggesting the CO_2 emission during CS combustion is increasing. The region of 4000–3500 cm^{-1} represents the generation of H_2O. The production of SO_2 is monitored in the region of 1342 cm^{-1}, due to the decomposition of organic and inorganic compounds containing sulfur in the samples.

Since the main component of coal is carbon, most of the gas products are released in the form of CO_2 during the combustion process. When the coal was started to be heated at a certain heating rate, the FTIR spectra began to collect and analyze the evolved gaseous products. The CO_2 gases from TGA passed through a transfer line into the FTIR spectrometer for further analysis. Thus, FTIR monitored continuously the time dependent evolution of CO_2 products. A linear relation between spectral absorbance at a given wavenumber and concentration of gaseous components is given by Beer's Law. In this study, the points of absorbance at a certain wavenumber were plotted against time in order to obtain a formation profile for CO_2 observed in the spectra during experiments. The generation of CO_2 with the time at the wavenumber of 2358 cm^{-1} is displayed in Fig. 9. There is one CO_2 evolution main peak for RC, CS and CG, and the corresponding temperatures for each other are 580 °C, 572 °C and 588 °C, respectively. It corresponds to the volatile decomposition, fixed carbon combustion and the solid residue decomposition step observed in the thermogravimetric analysis. The formation CO_2 profile of CG shifts to higher temperature zone as higher ash content. This leads to slower burning and later release of CO_2. The CO_2 absorption peak of CS is much higher than that of CG and RC. The different chemical compositions of CS, RC, and CG, such as higher fixed carbon and lower ash compositions in CS, may lead to more CO_2 emission during combustion. From the evolution curves, the integral values (I) under the time-dependent evolution curves of CO_2 were calculated, the results are ranked as: CS (121.8)> RC (105.7)> CG (63.6).

Fig. 10 illustrates the results of orthogonal experiments on CO_2 emission of blends of CS, CG and RC. The integral values of the mixed samples are all below 80, which are much lower than those of CS and RC. It reveals the reduction of CO_2 by mixing method. When the mixing ratio of CS:RC:CG = 20:40:40, I is 29% smaller than that of individual CG. With increasing the proportion of CS from 20% to 60%, I increases by 9%. With increasing CS ratio from 60% to 80% further, I increases by 21%. It is known that the positive synergistic interactions occur and influence the CO_2 emission behavior during the combustion of blends, leading to the combustion of coal blends that cannot be estimated from the behavior of mono-combustion. The experimental CO_2 integral values are about 50% lower than anticipated, indicating that co-combustion inhibited the emission of CO_2 from the blends. Moreover, I reduces to 30 when the O_2 concentration is 40%. When the heating rate increases from 10 to 30 °C/min, I increases by 3.3 times. Increasing the heating rate can strengthen the effect on the coal structure, so that the chemical bond in coal unit is cracked rapidly

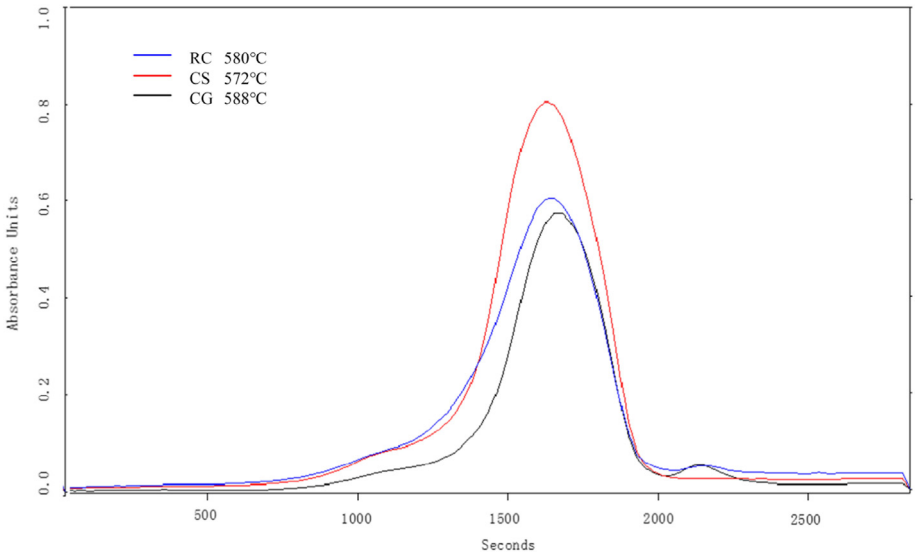

Fig. 9. Evolution of CO_2 with time in the combustion of RC, CS and CG.

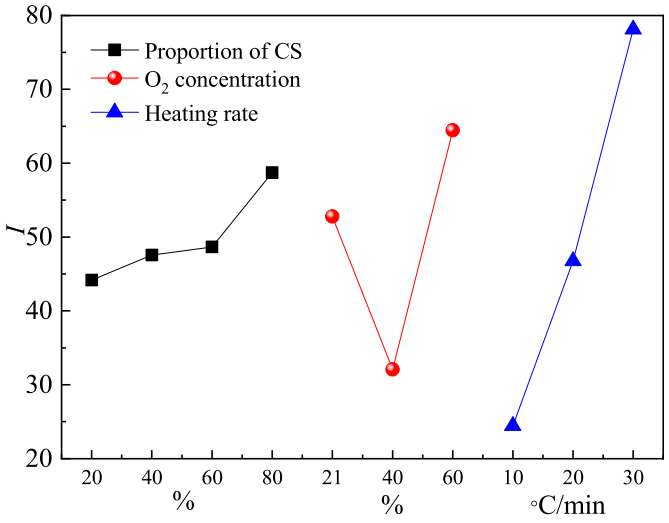

Fig. 10. Orthogonal experiments on CO_2 emission of blends of CS, CG and RC.

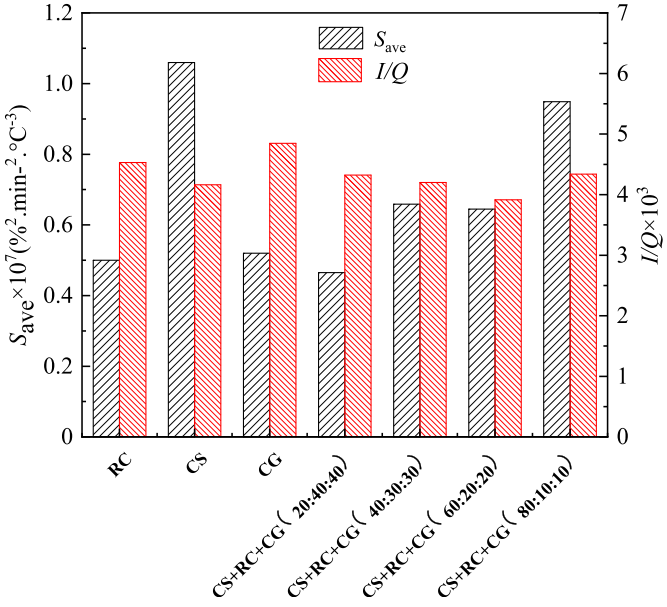

Fig. 11. S_{ave} and I/Q of RC, CS, CG and their blends.

and more CO_2 is generated at high temperature. Based on the CO_2 integral value in Fig.10 and 20%, 40% and 10 °C/min are the optimum levels for the proportion of CS, O_2 concentration and heating rate, respectively.

3.4. Determination of mixing ratio of RC, CS and CG

The above analysis results show that the mixture of RC, CS and CG is beneficial for the combustion and reducing CO_2 emission. Thus, in order to determine the optimal mixing ratio of RC, CS and CG in a CFB boiler, a novel index defined as the CO_2 integral value of per unit calorific (I/Q) for fuels was calculated. Factors including volatile content, ash properties contribute to the synergistic interactions between RC, CS and CG. Each factor affects the combustion behavior and CO_2 emission to some extent. It is necessary to develop a novel index, which can be applied to different types of fuel. Therefore, the low heat value, which has direct reflection on fuel properties, is presented as the parameter for the novel index. This index could be used in the selection of optimal mixing ratio for multi-coal in CFB plants aiming at improving the combustion performance of low heat value coals as well as reducing original CO_2 emissions. The results are shown in the Fig. 11. When the mixing ratio of CS:RC:CG = 60:20:20, I/Q reduces to 3900. As increasing CS from 60% to 80%, this index increases by 10.8%, whereas S_{ave} increases by 47%. Considering the improvement in the combustion performance and the CO_2 emission, the mixing ratio of CS:RC:CG = 80:10:10 is recommended. Therefore, the potential global optimum blending ratio of CS is 80%, O_2 concentration and heating rate for co-combustion of the mixtures are 40% and 30 °C/min, respectively. The further investigation of the blend (CS:RC:CG = 80:10:10) in a large-scale fluidized bed boiler is necessary. Moreover, the O_2 concentration may be extended to more ranges according to the industrial application conditions. For example, the O_2 concentration of coal combustion usually kept at 4%–6% in a CFB boiler.

4. Conclusions

The combustion characteristics and CO_2 emission behaviors of coal slime, coal gangue, raw coal and their mixtures were obtained according to TG-FTIR analysis. The co-combustion method could avoid the drawbacks of individual fuel, improve combustion performances and reduce CO_2 emissions. The effects of proportion of CS, O_2 concentration and heating rate were discussed by orthogonal experiments. The results provide a novel index (I/Q) to quantify the CO_2 emission of multi-fuels during cofiring which is a reference for further application in a circulating fluidized bed boiler. The main conclusions are summarized as follows:

(1) Ignition temperature (T_i), burnout temperature (T_f) and comprehensive combustion characteristic index (S) are important parameters to evaluate the combustion characters of multi-fuels. By mixing method, the ignition and burnout temperature both become lower. S_{ave} increases by 2.1 times with the ascent of CS ration from 20% to 80%. As the heating rate increases, S_{ave} become correspondingly higher.
(2) There is positive synergistic interaction between CS, CG and RC during co-combustion process. At 450–700 °C, it shows a significant promoting effect because of the thermal effect and the catalytic activity of minerals in ash. The activation energy values of samples are obtained by the Coats-Redfern method. It concludes that E-exp of each mixed fuel is lower than E-cal, which further illustrates the presence of interactions. It needs to note that there is a sharp fall of the activation energy with the increase of heating rate.
(3) Four gaseous generation peak and typical groups of CO_2, H_2O, CO and SO_2 are discovered in the IR spectrum. The CO_2 integral value of CS is 15% and 92% higher than that of RC and CG, respectively. The blending method contributes a lot in reducing the emission of CO_2. The integral value under the evolution curves of CO_2 reduces to 30 when the O_2 concentration is 40%.
(4) Considering the better combustion characteristics and lower CO_2 emission, the potential global optimum blending ratio of CS is 80%, O_2 concentration and heating rate for co-combustion of the mixtures are 40% and 30 °C/min, respectively.

Credit author statement

Zhangke Ma: Methodology, Data curation, Writing – original draft. **Leming Cheng:** Conceptualization, Validation, Writing – review & editing, Supervision. **Qinhui Wang:** Resources. **Liyao Li:** Visualization. **Guanwen Luo:** Validation. **Weiguo Zhang:** Formal analysis.

Declaration of competing interest

The authors declare that they have no known competing financial interests or personal relationships that could have appeared to influence the work reported in this paper.

Acknowledgment

This work was supported by the National Key R&D Program of China (2020YFB0606201).

References

[1] Zhao C, Luo K. Sulfur, arsenic, fluorine and mercury emissions resulting from coal-washing byproducts: a critical component of China's emission inventory. Atmos Environ 2017;152:270–8.
[2] Cen K, Ni M, Chi Y, et al. Recent advances of coal washery sludge fluidized bed combustion technology. In: Proceedings of the 12th international conference on fluidized bed combustion; 1993. p. 361–6.
[3] Liao X, Zhang S, Wang X, et al. Co-combustion of wheat straw and camphor wood with coal slime: thermal behaviour, kinetics, and gaseous pollutant emission characteristics. Energy 2021;234:121292.
[4] Wu G, Wang T, Wang J, et al. Occurrence forms of rare earth elements in coal and coal gangue and their combustion products. J Fuel Chem Technol 2020;48:1498–505.
[5] Zhang Y, Guo Y, Cheng F, et al. Investigation of combustion characteristics and kinetics of coal gangue with different feedstock properties by thermogravimetric analysis. Thermochim Acta 2015;614:137–48.
[6] Li W. Study on the co-combustion and pollutant emission characteristics of coal gangue and coal slime in O_2/CO_2. Taiyuan: Shanxi University; 2018. p. 13–23.
[7] Gani A, Wattimena Y, Erdiwansyah, Mahidin, Muhibbuddin, Riza M. Simultaneous sulfur dioxide and mercury removal during low-rank coal combustion by natural zeolite. Heliyon 2021;7:07052.
[8] Cheng L, Ji J, Wei Y, et al. A note on large-size supercritical CFB technology development. Powder Technol 2020;363:398–407.
[9] Su S, Pohl JH, Holcombe D, et al. Techniques to determine ignition, flame stability and burnout of blended coals in pf power station boilers. Prog Energy Combust Sci 2001;27:75–98.
[10] Duan L, Liu D, Chen X, et al. Fly ash recirculation by bottom feeding on a circulating fluidized bed boiler co-burning coal sludge and coal. Appl Energy 2012;95:295–9.
[11] Fu B, Liu G, Mian M, et al. Co-combustion of industrial coal slurry and sewage sludge: thermochemical and emission behavior of heavy metals. Chemosphere 2019;233:440–51.
[12] Huang Z, Jiang J, Xu Z, et al. Research on CFB boiler large proportion coal slime co-combustion test. Proc CSEE 2013;(S1):112–6.
[13] Min F, Zhang Z, Fan X, et al. Study on combustibility of slime from coal preparation plant. J China Coal Soc 2004;(2):216–21.
[14] Zhuang X, Song Y, Zhan H, et al. Synergistic effects in co-combusting of hydrochar derived from sewage sludge with different-rank coals. J Fuel Chem Technol 2018;46(12):1437–46.
[15] Gil MV, Casal D, Pevida C, et al. Thermal behavior and kinetics of coal/biomass blends during co-combustion. Bioresour Technol 2010;101(14):5601–8.
[16] Nyashina GS, Vershinina KY, Shlegel NE, et al. Effective incineration of fuel-waste slurries from several related industries. Environ Res 2019;176:108559.
[17] Wang F, Zhao J, Zhang Y. etal. Investigation of agglomeration process of coal slime used in fluidized bed combustion. Clean Coal Technol 2019;25(4):106–10.
[18] Fan H, Deng B, Shi J, et al. Experimental research on morphology and drying characteristics of coal slime dough injected into circulating fluidized bed boiler. Fuel Process Technol 2021;222:106981.
[19] Loboda EL, Yakimov AS. Some results of mathematical simulation of the process of peat ignition. High Temp 2013;51:841–8.
[20] Wang H, Liu S, Wang X, et al. Ignition and combustion behaviors of coal slime in air. Energy Fuels 2017;31:11439–47.
[21] Omar KI, Hossain I, Begum JA. Burning characteristics of high-ash bangladeshi peat. Int J Energy Res 1995;19:391–6.
[22] Song D, Wang Q, Shuang W, et al. Study on combustion characteristic of the North-Sichuan low-calorific-value coal gangue. Appl Chem Ind 2014;43:1784–7.
[23] Skodras G, Grammelis P, Basinas P. Pyrolysis and combustion behaviour of coal-MBM blends. Bioresour Technol 2007;98:1–8.
[24] Wang C, Wang F, Yang Q, R, et al. Thermogravimetric studies of the behavior of wheat straw with added coal during combustion. Biomass Bioenergy 2009;33:50–6.
[25] Cheng R, Wei X, Zhou L, et al. Experimental research on combustion and kinetic characteristics between coal slime and raw Coal. Therm Power Gener 2021;50:55–61.
[26] Jiang H, Gong D, Wang Z, et al. Experimental analysis on combustion characteristics of blended coal slime. J Guizhou Univ (Nat Sci) 2018;35:70–5.
[27] Liao X, Zhang S, Zhang X, et al. Interaction and kinetics during the co-combustion process of coal slime, coal gangue and slack coal. J China Coal Soc 2020:1–11.
[28] Oladejo JM, Adegbite S, Pang CH, et al. A novel index for the study of synergistic effects during the co-processing of coal and biomass. Appl Energy 2017;188:215–25.
[29] Huang X, Jiang X, Han X, et al. Combustion characteristics of fine- and micro-pulverized coal in the mixture of O_2/CO_2. Energy Fuel 2008;22:3756–62.
[30] Onenc S, Retschitzegger S, Evic N, et al. Characteristics and synergistic effects of co-combustion of carbonaceous wastes with coal. Waste Manag 2018;71:192–9.

[31] Ma L, Wang T, Liu J, et al. Effect of different conditions on the combustion interactions of blended coals in O_2/CO_2 mixtures. J Energy Inst 2019;92:413–27.
[32] Fan Y, Yu Z, Fang S, et al. Investigation on the co-combustion of oil shale and municipal solid waste by using thermogravimetric analysis. Energy Convers Manag 2016;117:367–74.
[33] Liu Y, Wu R, Yang P, et al. Parameter study of the injection configuration in a zero boil-off hydrogen storage tank using orthogonal test design. Appl Therm Eng 2016;109:283–94.
[34] Niu SL, Lu CM, Han KH, et al. Thermogravimetric analysis of combustion characteristics and kinetic parameters of pulverized coals in oxy-fuel atmosphere. J Therm Anal Calorim 2009;98:267–74.
[35] Li B, Li Y, Sun H, et al. Thermochemical heat storage performance of Cao pellets fabricated by extrusion-spheronization under harsh calcination conditions. Energy Fuel 2020;34:6462–73.
[36] Liu J, Feng Z, Zhang B, et al. Comparison of two methods for analyzing the activation energy of coal combustion. J Power Eng 2006;26(1):121–4.
[37] Gil MV, Riaza J, Alvarez L, et al. Kinetic models for the oxy-fuel combustion of coal and coal/biomass blend chars obtained in N_2 and CO_2 atmospheres. Energy 2012;48:510–8.
[38] Yuzbasi NS, Selcuk N. Air and oxy-fuel combustion characteristics of biomass/lignite blends in TGA-FTIR. Fuel Process Technol 2011;92:1101–8.
[39] Wang Y, Jia L, Guo J, et al. Thermogravimetric analysis of co-combustion between municipal sewage sludge and coal slime: combustion characteristics, interaction and kinetics. Thermochim Acta 2021;706:179056.
[40] Ma L. Experimental and numerical studies on ignition promotion and burnout inhibition during blended coals combustion. Wuhan: Huazhong University of Science and Technology; 2018. p. 28–35.
[41] Xu J, Zhang X, Jin T. Effect of Fe_2O_3 and K_2CO_3 on combustion and catalytic mechanism analysis of high ash coal from huaibei mining area. Bull Chin Ceram Soc 2016;35(6):1841–6.